Dalton Transactions

ROYAL SOCIETY OF CHEMISTRY

PAPER

View Article Online
View Journal | View Issue

Cite this: *Dalton Trans.*, 2021, **50**, 7640

Autocatalytic photodegradation of [Ru(II)(2,2′-bipyridine)$_2$DAD]$^+$ (DADH = 1,2-dihydroxyanthracene-9,10-dione) by hydrogen peroxide under acidic aqueous conditions†

Lingli Zeng,[a] Dumitru Sirbu, [b] Nikolai V. Tkachenko [c] and Andrew C. Benniston *[a]

Received 23rd March 2021,
Accepted 3rd May 2021

DOI: 10.1039/d1dt00952d

rsc.li/dalton

As part of a continuing effort to identify ruthenium agents capable of the photorelease of anthraquinone-based ligands the complexes Δ/Λ-[Ru(bpy)$_2$DAD]$^+$ (bpy = 2,2′-bipyridine) were produced by the reaction of 1,2-dihydroxyanthracene-9,10-dione (DADH) with chirally pure Δ/Λ-[Ru(bpy)$_2$(py)$_2$][(+)-*O*,*O*′-dibenzoyl-D-tartrate]·12H$_2$O (py = pyridine). A very subtle difference in the chemical shift of the hydroxyl proton in their high-field ^{1}H NMR spectra was observed, supporting that the OH proton is susceptible to a small change in environment at the metal centre. The excited state lifetime of the complexes, as measured by femtosecond pump–probe spectroscopy, was 7.1 (±0.8) ps in water (pH 2) and 13 (±1) ps in MeCN. Illumination of a sample of Λ-[Ru(bpy)$_2$DAD]$^+$ in water (pH 2) in the presence of hydrogen peroxide resulted in decomposition of the complex. The decay profile, as monitored at several wavelengths, was sigmoidal indicating the reaction was autocatalytic, in which the product formed catalysed decomposition of the starting complex. A mechanism is proposed that relies on participation of the uncoordinated hydroxyl group on the anthraquinone ligand in promoting water loss and radical formation in the excited state. The radical is oxidised by peroxide to generate the ruthenium(III) complex, which behaves as an oxidant in the autocatalytic process.

Introduction

Anthraquinone and its derivatives are ubiquitous in nature especially in plants[1] and serve several fundamentally important purposes.[2] They are generally found attached to sugars (*e.g.*, glycosides) in a living plant, and are often associated with electrochemical reactions by utilising the rich redox at the carbonyl sites. Anthraquinones play important roles in several types of medications and have been linked to benefits from their properties which include antibacterial, antifungal, antioxidant and antiviral. Within the plethora of anthraquinones is the compound 1,2-dihydoxyanthracene-9,10-dione (**DADH**), which is more commonly known as alizarin.[3] The compound is interesting in that it is not only a paint pigment but it has also found applications as a drug for the treatment of tumors.[4] Additionally, alizarin is important for its use as a staining agent in biological and geological research, specifically for colorimetric quantification of calcium.[5] The presence of the three adjacent oxygen groups opens up the opportunity for the compound to coordinate metal ions, noting that linkage isomers are possible depending on which oxygen pair donate to the metal ion centre. Previous work by Lever *et al.*[6] showed that linkage isomerization was pH dependent in the complex [Ru(II)(2,2′-bipyridine)$_2$alizarin]$^+$, which for simplicity is now referred to as **RDAD**. The interchange between the isomers results in a clear colour change. Despite the detailed redox chemistry of the complex, very little more is known about its photochemistry and stability. Our interest in the complex stemmed from previous work, which showed that the simpler version missing the 2-hydroxyl group could be decomposed in the presence of hydrogen peroxide and light.[7] It was not evident if the additional hydroxyl group would serve to promote or retard any photochemical reaction.

The current interest in photoactive complexes capable of releasing therapeutic[8] or cytotoxic agents[9] prompted the study of the complex **RDAD** (Scheme 1) under white light excitation

[a]*Molecular Photonics Laboratory, Chemistry-School of Natural & Environmental Sciences, Newcastle University, Newcastle upon Tyne, NE1 7RU, UK. E-mail: andrew.benniston@ncl.ac.uk*
[b]*School of Mathematics, Statistics and Physics, Newcastle University, Newcastle upon Tyne, NE1 7RU, UK*
[c]*Faculty of Engineering and Natural Sciences, Tampere University, P.O. Box 541, FI-33014 Tampere, Finland*

† Electronic supplementary information (ESI) available: NMR data, UV-vis decay data, pK_a plot. See DOI: 10.1039/d1dt00952d

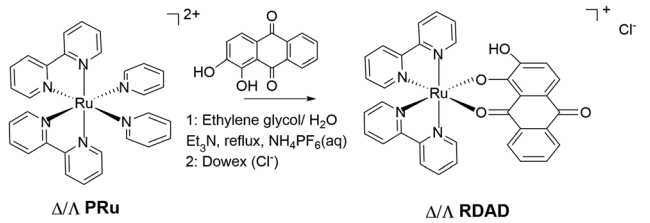

Scheme 1 Preparation of the ruthenium(II) polypyridyl complex of 1,2-dihydroxyanthracene-9,10-dione (**DADH**), also commercially known as alizarin.

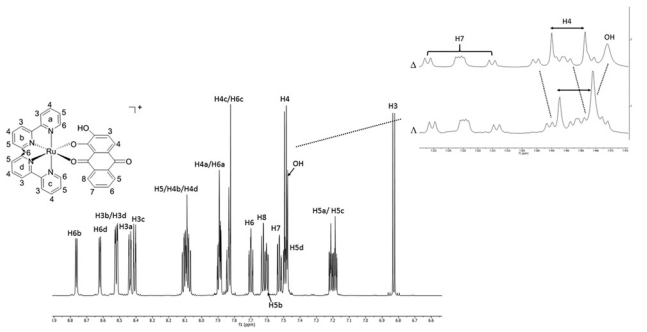

Fig. 1 A 700 MHz ^{1}H NMR spectrum of Δ-**RDAD** in CD_3CN showing the atomic labelling. Insert shows the expansion of the selected region and the comparison with the same region for Λ-**RDAD** in the same solvent.

in the presence of hydrogen peroxide. The primary focus was to elucidate if the alizarin was released from the complex, what other species would also be formed and the process for decomposition. As shown in our previous work, despite the extremely short excited state lifetime of *ca.* 7 ps the complex decomposed over some 100 minutes in acidic water containing peroxide under white light illumination. However, the reaction kinetics, as monitored by disappearance of the main absorption band at 580 nm, displayed behaviour typically observed for an autocatalytic process. This conduct was not observed previously, pointing to the fact that the hydroxyl group aids in the decomposition process. A simple mechanism is proposed based on participation of the 2-hydroxyl group, by elimination of water in the complex's excited state and oxidation by the peroxide present.

Results and discussion

Synthesis and characterization

The racemic synthesis of **RDAD** was published previously,[6] but not the corresponding chirally pure Δ and Λ forms. Although pure enantiomers are undoubtedly not critical for photodecomposition studies in achiral environments, they are potentially more interesting when bound in chiral environments; the obvious example being that of DNA and minor/major groove binding.[10] Hence, for completeness the two pure enantiomers were produced using the simple method developed by von Zelewsky and co-workers.[11]

The reflux of **DADH** in aqueous ethylene glycol with one equivalent of either Δ-**PRu** or Λ-**PRu** and triethylamine resulted in the formation of a purple solution. Dark purple solids were precipitated by the addition of KPF_6 (aq) and obtained in good yields of *ca.* 60% and high purity, as per high-performance liquid chromatography (HPLC, see ESI†). The hexafluorophosphate complexes were typically soluble in polar solvents such as acetone, acetonitrile and dimethylsulfoxide. Water soluble versions of the complexes were obtained by chloride anion exchange using Dowex. A low-resolution ^{1}H NMR spectrum for racemic **RDAD** was reported before,[12] and so for completion a high-resolution (700 MHz) spectrum for Δ-**RDAD** in CD_3CN is presented in Fig. 1. The assignment of the proton resonances was based on a ^{1}H–^{1}H COSY and HSQC spectra (see ESI†) and previous assignments in the literature. The complexity of the spectrum is partly a consequence of the low symmetry of the attached **DAD** ligand. The noted shifts of specific resonances are fully consistent with protons residing in close proximity to aromatic rings and their shielding ring currents. For instance, the protons H_{6a} and H_{6c} of the 2,2′-bipyridine ligands point towards aryl rings of the **DAD** ligand, whereas protons H_{6b} and H_{6d} point at pyridine groups. A significant difference is observed in the upfield chemical shifts between these two proton pairs. The proton H_8 for **DAD** is shifted upfield because of its close proximity to a pyridine ring.

A cursory inspection of the ^{1}H NMR spectra for Δ-**RDAD** and Λ-**RDAD** in CD_3CN suggested that they were identical. However, a closer examination of specific resonances revealed subtle differences between the two spectra as illustrated in the Fig. 1 insert. The most discernible difference is observed around 7.5 ppm corresponding to a region where there is a broad resonance for the hydroxyl group. This proton resonance is shifted downfield in Λ-**RDAD** compared to the other isomer, which is in fitting with it interacting to a lesser extent to the pyridine π-system, or more strongly hydrogen bonding to the proximal oxygen atom.

For brevity only the properties of one isomer Λ-**RDAD** will be described in the following sections. Limited experiments performed using Δ-**RDAD** afforded essentially the same results as for the other isomer.

Photophysical properties

An absorption spectrum of the chloride salt of Λ-**RDAD** in H_2O (pH = 2) is shown in Fig. 2. Based on earlier work the main absorption band located at λ_{max} = 567 nm (ε_{max} = 8990 M^{-1} cm^{-1}) is assigned to a metal-to-ligand charge-transfer (^{1}MLCT) band in which a single electron is promoted from the full t_{2g} set to a π*-orbital located on the anthraquinone-based ligand.[8] There is in addition a prominent long tail which stretches well into the red region, with contributions from the spin-forbidden singlet to triplet MLCT transition and intramolecular ligand–ligand charge transfer transition. The other major absorption profile located at λ_{MAX} = 472 nm (ε_{max} = 9150 M^{-1} cm^{-1}) is the ^{1}MLCT correlated with an electronic transition

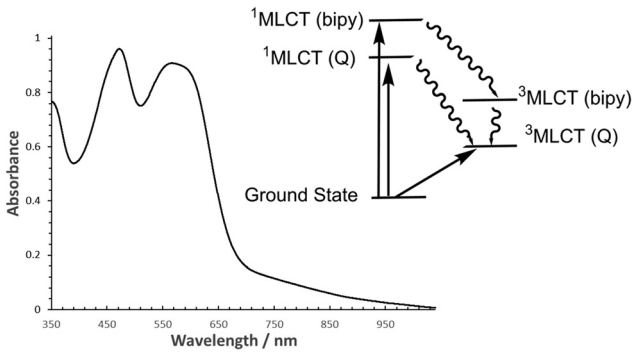

Fig. 2 Room temperature normalised absorption spectrum of Λ-**RDAD** in deionised H_2O (pH 2). Insert shows a simplified picture of excited states where labels in brackets identify the ligand associated with the electron localization. bipy = 2,2′-bipyridine, Q = anthraquinone ligand.

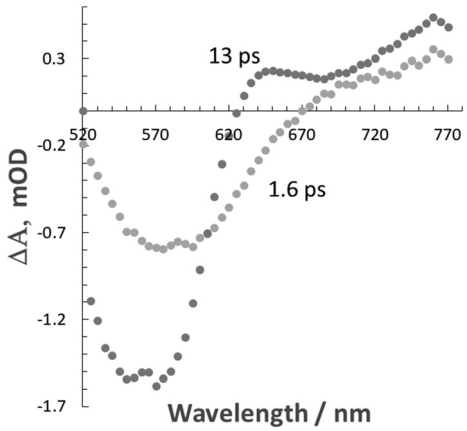

Fig. 3 Differential transient absorption spectra obtained from a global fit to two exponentials to pump probe data recorded for Λ-**RDAD** in MeCN.

from the ruthenium(II) centre to a 2,2′-bipyridine ligand. It should be noted that π–π* transitions for **DADH** also lie in the region between 400–500 nm. Within the pH range 2–10 the absorption spectrum for the complex did not change significantly. The observed modification in colour of the solution at high pH (>11) is consistent with deprotonation of the hydroxyl group as described previously in the literature (see ESI†).[6]

Although the free ligand **DADH** is slightly fluorescent in an aqueous solution[13] no reproducible emission could be seen for both isomers of **RDAD**, and as far as we are aware no room temperature phosphorescence was reported for the racemic complex. The excited state behaviour for ruthenium(II) polypyridyl complexes is well understood with the initially formed ^{1}MLCT state rapidly converting in a few femtoseconds to the ^{3}MLCT because of the heavy atom effect.[14] Applying the same process to **RDAD** would essentially generate a low-energy triplet state which can be formerly written as $[Ru(III)(bipy)_2DAD^{\bullet-}]^+$. As illustrated in the simplified picture in Fig. 2 it is reasonable to assume that formation of the bipyridine-based ^{1}MLCT state ($[Ru(III)(bipy)(bipy^{\bullet-})DAD]^+$) would also rapidly intersystem cross to its corresponding ^{3}MLCT state. The lack of room temperature phosphorescence, even from the upper-lying ^{3}MLCT state, would insinuate that internal conversion to the anthraquinone-based ^{3}MLCT state is efficient. This interpretation is not too unreasonable since previous calculations have shown that the frontier molecular orbitals for **RDAD** are not "pure" and that there is a mixing of states.[15]

The what appeared to be fast excited state decay in Λ-**RDAD** was more comprehensively studied using femtosecond pump–probe spectroscopy. Excitation of a sample in MeCN with a 100 fs laser pulse delivered at 500 nm produced a series of temporal profiles, which were globally fitted to two exponentials to produce two clear transient differential spectra (Fig. 3). The shortest lifetime component (1.6 ps) contains a feature that maps to the ground-state absorption profile and a positive transient profile at long wavelength. The slightly longer-lived transient profile (13 ps) is more pronounced in the long-wavelength region. Using the model proposed in Fig. 2 the 1.6 ps transient is assigned to the ^{3}MLCT (bipy) state and the 13 ps transient to the ^{3}MLCT (Q) state. The ultrashort lifetime is a result of fast non-radiative decay of the low-energy anthraquinone-based triplet state as predicted by the energy gap law.[16] Similar behaviour was previously reported for the analogous complex without the additional hydroxyl group.[7]

Transient absorption data were also collected under different conditions including in water and in the presence of H_2O_2. The data are presented in Table 1. There is distinct decrease in the two recorded lifetimes in changing from MeCN to H_2O, but the addition of hydrogen peroxide had no major affect.

Degradation studies

Given the ultrashort excited state lifetime for Λ-**RDAD**, and the lack of any sign of reaction with H_2O_2, the decomposition of the complex in water over some 100 minutes was unexpected but rewarding. As shown in Fig. 4 the irradiation of a dilute solution in water (pH 2) with white light resulted in clear alterations to the absorption spectrum. The absorption bands associated with both the ^{1}MCLT states decreased over time and there was sign of a new weak absorption band at *ca.* 960 nm. A similar experiment performed in the dark showed no obvious alterations. The final spectrum closely resembled that produced by *in situ* oxidation of Λ-**RDAD** using PbO_2 (see

Table 1 Conditions and calculated parameters from femtosecond pump–probe spectroscopy experiments for Λ-**RDAD**

Solvent and conditions	Lifetimes/ps[c]
H_2O/pH 2	τ_1 = 0.9 (0.2), τ_2 = 7.1 (0.8)
H_2O/pH 2/0.3% H_2O_2[a]	τ_1 = 1.1 (0.4), τ_2 = 11 (2)
H_2O/pH 2/1% H_2O_2[a]	τ_1 = 1.0 (0.4), τ_2 = 9 (2)
MeCN[b]	τ_1 = 1.6 (0.3), τ_2 = 13 (1)

[a] Percentage as volume per volume. [b] As the PF_6^- salt. [c] Error in bracket.

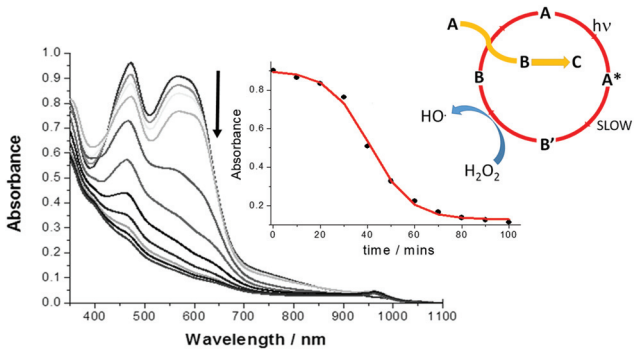

Fig. 4 White light induced alterations to the absorption spectra of Λ-**RDAD** (conc. = 0.1 mM) in N_2-purged deionised water (pH 2) containing H_2O_2 (0.4 M) over 100 minutes. The inserts show the change in absorbance monitored at 580 nm over time and the least-squares sigmoidal fit to the equation for an autocatalytic reaction and the proposed process where **A**, **B′** and **B** are defined in Scheme 2.

ESI†).[17] The loss of the ^{1}MLCT absorption band at 567 nm is consistent with formation of $[Ru(III)(bipy)_2DAD]^{2+}$ and eventually the removal of **DAD** from the coordination sphere.

The decay of the complex as monitored at several wavelengths between 440–580 nm displayed a sigmoidal profile as shown in the insert of Fig. 4. This type of behaviour is typical for an autocatalytic process in which the product formed catalyses the starting material decomposition (eqn (1)), where k_1 is the rate constant for the non-catalytic reaction and k_2 is the rate constant for the catalytic reaction.[18]

$$\text{Rate} = k_1[\text{Reactant}] + k_2[\text{Reactant}][\text{Product}] \quad (1)$$

The sigmoidal plot was analysed using a least-squares fit to eqn (2) which represents the change in concentration of the reactant [R] over time (t) in terms of k_1 and k_2 and its initial concentration $[R_0]$.

$$[R] = \frac{\left(\frac{k_1}{k_2}\right) + [R_0]}{1 + \left(\frac{k_1}{k_2[R_0]}\right)\exp[(k_1 + k_2[R])t]} \quad (2)$$

The average values from fits at the different wavelengths are $k_1 = 1.2 \pm 0.1 \times 10^{-3}$ min^{-1} and $k_2 = 1019 \pm 200$ M^{-1} min^{-1}. By monitoring the absorption profile at longer wavelength (>600 nm) the initial slow induction period was far more obvious and almost constant, and the faster process displayed a decay which could be fitted to a single exponential. The average fitted lifetime $\tau_2 = 19 \pm 3$ min, corresponding to a first-order rate constant of 52.6×10^{-3} min^{-1}. Noting that $1/(\tau_2 \times k_2)$ has units of concentration this equates to *ca.* 5×10^{-5} M corresponding to half the concentration of the initial solution. A series of similar light-induced degradation experiments were also performed at different pH up to 7 (see ESI†) and the results from the analysis are collected in Table 2.

Table 2 Parameters obtained from a least-squares fit to eqn (2) using changes to the absorption spectra during decomposition

pH	$k_1 \times 10^{-3}$ [a]/min^{-1}	k_2/M^{-1} [a] min^{-1}	τ_2/min
2	1.2 ± 0.1	1019 ± 200	19 ± 3
3	3.3 ± 0.6	396 ± 60	31 ± 3
4	3.1 ± 0.4	438 ± 56	28 ± 2
5	10.9 ± 1.5	238 ± 40	30 ± 3
6	11.0 ± 1.1	231 ± 35	30 ± 3
7	11.0 ± 1.1	233 ± 34	30 ± 3

[a] Average value using 16 different wavelengths.

Proposed decay process

The catalytic reaction appears to be dominant at low pH and the rate constants tend toward a fixed value between pH 5–7. The pH trend observed for k_1 is characteristic for an excited state process that relies on protonation, and from the pH dependence plot (see ESI†) the pK_a is around 4.3. The protonated form of anthraquinone (AQH) has a pK_a of around −8.5 in water[19] whereas the pK_a for the conjugate acid of $AQ^{\bullet-}$ is *ca.* 5.3.[20] Given these values it is unlikely that the ground-state complex will be protonated, but it is more probable in the excited state since C–$O^{\bullet-}$ is formerly produced (Scheme 2). A further protonation at this site opens up a decay pathway which may help explain the catalytic reaction. A loss of a water molecule is feasible as promoted by electron pair donation from the distal hydroxyl group as shown. This process is not accessible in the similar ruthenium complex supporting the non-hydroxyl version of the ligand as reported previously.[7] Deprotonation would leave a quinoid-based ligand as its radical, which can be oxidised by the peroxide present to form the ruthenium(III) complex which is itself an oxidant. It is worth mentioning that the one electron reduction of hydrogen peroxide would also create the strongly oxidising hydroxyl radical (eqn (3) & (4)).[21] The participation of the hydroxyl radical in facilitating oxidation of the ground-state complex cannot be ruled out.

$$H_2O_2 + H^+ + e^- \rightleftharpoons HO^{\bullet} + H_2O \quad E^\circ = +0.80\,\text{V}(vs.\,\text{NHE}) \quad (3)$$

$$HO^{\bullet} + H^+ + e^- \rightleftharpoons H_2O \quad E^\circ = +2.73\ \text{V}\ (vs.\ \text{NHE}) \quad (4)$$

It should be also mentioned that the dominant photoprocesses are illustrated in the top part of Scheme 2, and that the proposed peroxide-based reaction is a minor side reaction. This assumption appears reasonable since the proposed ruthenium(III) complex must firstly build-up to promote the autocatalytic reaction. The overall process is summarised in the insert of Fig. 4, where **A** is the starting complex and **B′** and **B** are the ruthenium(III) complexes illustrated in Scheme 2. The redox reaction of **A** with **B** represents a self-exchange process, noting that cyclic nature of the reaction is broken when **B** further degrades by loss of the anthraquinone-based ligand.

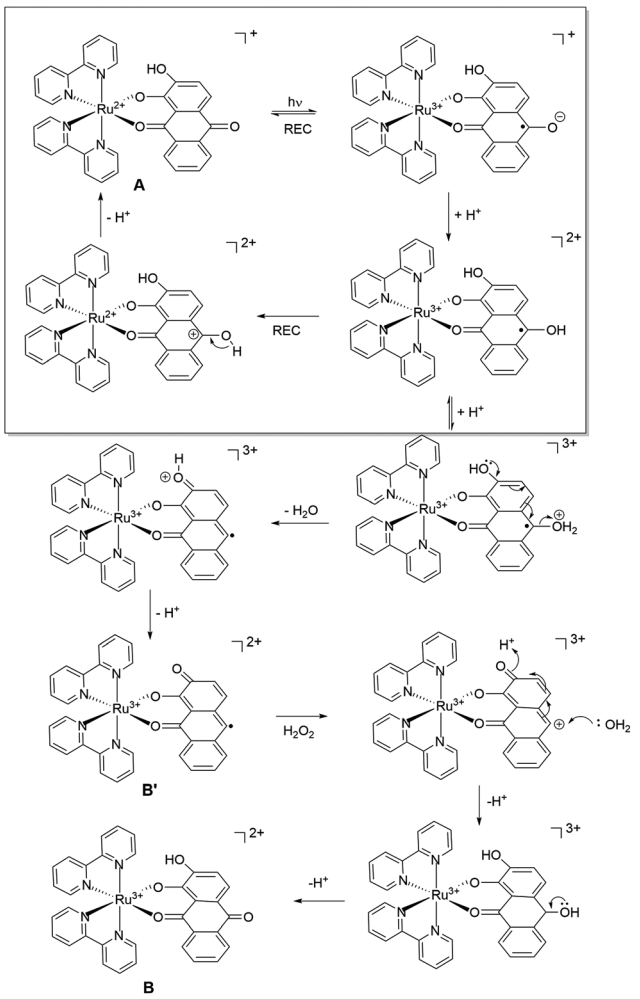

Scheme 2 Proposed processes following excitation of Δ/Λ-**RDAD** in acidic water in the presence of hydrogen peroxide. The top part of the scheme depicts the dominant processes that occur within the several picoseconds time window. The bottom part is a minor pathway as promoted by protonation and water loss. The labels refer to the cyclic scheme shown in Fig. 4.

Conclusions

Notwithstanding the ultrashort lifetime of **RDAD** the decomposition of the complex is achievable under white light excitation in the presence of hydrogen peroxide, releasing in the reaction the anthraquinone-based ligand. The autocatalytic process which facilitates the photoreaction would appear to be an advantageous way to enhance ligand loss, especially in quinone-based ligands that contain an additional OH group that is not employed in metal ion binding. This structure–reactivity relationship could be readily studied, especially focusing on the substitution position of the hydroxyl group and the autocatalytic behaviour. There are several anthraquinone compounds, such as emodin and chyrsophanol, which may display a similar release mechanism when complexed to a "Ru(II)(bipy)$_2$" core. There is current interest in the photorelease of agents in cells and tumours for photodynamic therapy applications, and the release of anthraquinone compounds at specific sites may pave the way forward for targeted treatments. Alazarin, for example, is known to significantly and strongly impair both osteosarcoma and breast cancer tumorigenesis.[22] The utilization of natural *in situ* oxidants (or reductants) coupled to autocatalysis in cells to enhance the photorelease of agents[23] is a promising strategy that warrants further exploration.

Experimental

All the chemicals were purchased from commercial sources and used as received without further purification. The complexes Δ/Λ-[Ru(bipy)$_2$(py)$_2$][(+)-*O*,*O*′-dibenzoyl-D-tartrate]·12H$_2$O were prepared by the method of von Zelewsky.[11] For the studies undertaken in water, ruthenium hexafluorophosphate salts were converted to chloride salts by using Amberlite® IRA-410 chloride form. Aqueous solutions were prepared using a PURELAB® Option-Q water purification system. High-field nuclear magnetic resonance (NMR) spectra including ^{1}H-NMR, ^{13}C-NMR, COSY, HSQC, HMBC were collected on a Bruker Advance III HD 700 MHz spectrometer. Chemical shifts for all complexes were reported relative to acetonitrile-d^3 (Cambridge Isotope Laboratories, CD$_3$CN, 99.8%) at δ = 1.940 ppm. FT-IR spectra were recorded on a PerkinElmer FT-IR Spectrum Two spectrometer. Chromatography experiments were performed on Agilent 1260 Infinity HPLC system equipped with Raptor C18 column (100 × 3 mm; 2.7 μm particle size) using water/acetonitrile 1/9 mixture as eluent (0.3 mL min^{-1}) and compared to the solvent blank run. Diode Array Detector (1260 DAD VL+) was fixed in the spectral region of interest at 567 nm and at 250 nm to detect any non-photoactive impurities. High-resolution electron spin ionization (ESI) mass spectrometry was collected by National Mass Spectrometry Facility (NMSF) in Swansea.

Preparation of Λ-RDAD

To a solution of Λ-[Ru(bipy)$_2$(py)$_2$][(−)-*O*,*O*′-dibenzoyl-L-tartrate]·12H$_2$O (114.4 mg, 0.1 mmol, 1 eq.) in ethylene glycol : H$_2$O (5 : 1, 30 mL) was added alizarin (24 mg, 0.1 mmol, 1 eq.) and triethylamine (0.030 mL, 0.2 mmol, 2 eq.). The reaction mixture was shielded from light, stirred and heated at 120 °C under a nitrogen atmosphere for 4 h until all the starting material was consumed during which time the solution changed from orange to dark-red. The solution was cooled down to R.T. and **Λ-RDAD** was precipitated by addition of excess KPF$_6$ from water. The black compound was collected by filtration and rinsed with distilled water and allowed to air dry overnight. ^{1}H NMR (700 MHz, acetonitrile-d_3) δ (ppm) = 8.76 (d, J = 5.3 Hz, 1H, 2,2′-bipyridyl), 8.62 (d, J = 5.8 Hz, 1H, 2,2′-bipyridyl), 8.52 (d, J = 8.2 Hz, 2H, 2,2′-bipyridyl), 8.42 (d, 1H, J = 8.4 Hz, 2,2′-bipyridyl), 8.41 (d, J = 8.5 Hz, 1H, 2,2′-bipyridyl), 8.14–8.02 (m, 3H, 2,2′-bipyridyl and alizarin ligand), 7.92–7.86 (m, 2H, 2,2′-bipyridyl), 7.86–7.78 (m, 2H, 2,2′-bipyridyl), 7.70 (t, 1H, J = 7.6 Hz, alizarin ligand), 7.62

(d, 1H, J = 8.2 Hz, alizarin ligand), 7.60 (t, 1H, J = 6.5 Hz, 2,2′-bipyridyl), 7.53 (t, 1H, J = 8.0 Hz, alizarin ligand), 7.51–7.45 (m, 3H, 2,2′-bipyridyl and alizarin ligand), 7.21 (t, 1H, J = 6.5 Hz, 2,2′-bipyridyl), 7.18 (t, 1H, J = 6.5 Hz, 2,2′-bipyridyl), 6.83 (d, 1H, J = 8.0 Hz, alizarin ligand). ^{13}C NMR (176 MHz, acetonitrile-d_3) δ 182.57, 180.06, 160.55, 159.89, 159.70, 159.07, 158.85, 158.60, 155.39, 155.01, 151.27, 151.08, 138.94, 138.50, 137.12, 136.77, 136.37, 134.89, 133.68, 133.06, 128.12, 127.91, 127.76, 127.74, 126.87, 126.68, 125.94, 124.68, 124.60, 124.59, 124.53, 122.38, 117.87, 112.90; FT-IR (cm^{-1}) 431 w, 452 w, 556 s, 599 m, 648 w, 659 m, 668 w, 709 s, 728 s, 758 s, 831 vs, 877 w, 970 w, 1022 s, 1037 w, 1056 w, 1068 w, 1094 w, 1105 w, 1123 w, 1158 m, 1189 m, 1223 m, 1243 m, 1260 s, 1305 s, 1322 w, 1371 m, 1401 m, 1421 m, 1444 m, 1461 m, 1481 w, 1508 s, 1537 m, 1584 w, 1594 w, 1603 w, 1644 m, 1716 vw, 2853 w, 2924 w, 2955 w, 3075 w, 3357 vw br, 3585 vw, 3648 vw; NSI-FTMS (m/z): found [M − PF_6^+]: found 653.0745, calcd for $C_{34}H_{23}N_4O_4Ru$: 653.0767; HPLC (min): 9.25.

Preparation of Δ-RDAD

This followed the preparation of **Λ-RDAD** but Δ-[Ru(bipy)$_2$(py)$_2$][(+)-*O*,*O*′-dibenzoyl-D-tartrate]·12H$_2$O was used as the precursor. ^{1}H NMR (700 MHz, acetonitrile-d_3) δ (ppm) = 8.76 (d, J = 5.5 Hz, 1H, 2,2′-bipyridyl), 8.62 (d, J = 5.6 Hz, 1H, 2,2′-bipyridyl), 8.52 (d, J = 8.1 Hz, 2H, 2,2′-bipyridyl), 8.42 (d, J = 8.4 Hz, 1H, 2,2′-bipyridyl), 8.41 (d, J = 8.1 Hz, 1H, 2,2′-bipyridyl), 8.14–8.05 (m, 3H, 2,2′-bipyridyl and alizarin ligand), 7.95–7.87 (m, 2H, 2,2′-bipyridyl), 7.87–7.81 (m, 2H, 2,2′-bipyridyl), 7.70 (t, J = 7.6 Hz, 1H, alizarin ligand), 7.63 (d, J = 8.0 Hz, 1H, alizarin ligand), 7.61 (t, 1H, J = 6.5 Hz, 2,2′-bipyridyl), 7.55 (t, J = 7.6 Hz, 1H, alizarin ligand), 7.50–7.47 (m, 3H, 2,2′-bipyridyl and alizarin ligand), 7.21 (t, J = 7.6 Hz, 1H, 2,2′-bipyridyl), 7.19 (t, J = 6.8 Hz, 1H, 2,2′-bipyridyl), 6.83 (d, J = 7.9 Hz, 1H, alizarin ligand). ^{13}C NMR (176 MHz, acetonitrile-d_3) δ 182.12, 179.68, 160.15, 159.49, 159.29, 158.66, 158.44, 158.17, 154.99, 154.61, 150.88, 150.69, 138.52, 138.09, 136.66, 136.35, 135.96, 134.46, 133.31, 132.67, 127.72, 127.50, 127.36, 127.35, 126.45, 126.27, 125.54, 124.27, 124.19, 124.18, 124.11, 121.94, 117.46, 112.51; FT-IR (cm^{-1}) 431 w, 452 w, 556 s, 599 m, 648 w, 659 m, 668 w, 709 s, 728 s, 758 s, 830 vs, 877 w, 970 w, 1022 s, 1037 w, 1056 w, 1068 w, 1094 w, 1105 w, 1123 w, 1158 m, 1188 m, 1223 m, 1243 m, 1260 s, 1305 s, 1322 w, 1371 m, 1401 m, 1421 m, 1444 m, 1461 m, 1481 w, 1508 s, 1537 m, 1584 w, 1594 w, 1603 w, 1644 m, 1732 vw, 2852 vw, 2922 vw, 2963 vw, 3075 vw, 3369 vw br, 3587 vw, 3648 vw; NSI-FTMS (m/z): found [M − PF_6^+]: found 653.0740, calcd for $C_{34}H_{23}N_4O_4Ru$: 653.0767; HPLC (min): 9.31.

Photochemical kinetic experiments

UV–visible absorption properties under different conditions were collected on Shimadzu Spectrophotometer UV-1800 at a resolution of 0.5 nm with medium scan speed from range 300–1100 nm. For stability and photobleaching test, solar simulators calibrated with an AM 1.5G filter and equipped with a 150 W Xe lamp (SS-150 Series, Sciencetech Inc.) was used as the light source. A stability test of **RDAD** was carried out in CH_3CN and distilled water (pH = 7) within few hours. The temperature of the cell was maintained constant at 20 °C.

Photochemical degradation test

For the degradation kinetic studies, pH 2–13 aqueous solutions were used. The pH values were measured using a Jenway 3310 pH meter, utilizing a three point calibration with pH = 4.0, 7.0, and 10.0 buffer solutions. For all solutions the pH in time was measured and adjusted as necessary to keep it constant. The photochemical degradation reactions were initiated by adding freshly prepared 0.4 M H_2O_2 to 1 × 10^{-4} M **RDAD** aqueous solution with different pHs. The solution was bubbled with N_2 for few minutes and irradiated under white light at R.T. At an appropriate time intervals, samples were taken and their UV-Vis absorption spectra were measured. All kinetic experiments were performed in duplicate.

Transient absorption spectroscopy

Excited state dynamic processes in femtoseconds to nanoseconds timescales were studied using the pump–probe method as described in detail elsewhere.[24] The fundamental light source at 800 nm was generated by a Ti:sapphire laser system (Libra F laser system, Coherent Inc.) which produced 1 mJ pulses with duration 100 fs at a 1 kHz repetition rate. Majority (~90%) of the fundamental beam power was delivered to Optical Parametric Amplifier (OPA) (TOPAS C, Light Conversion Ltd) and was tuned to generate pump pulses at 410, 470 or 500 nm for **RDAD**. The pump beam diameter at the sample was around 0.5 mm and the power was attenuated by optical filters to excitation density at the sample <0.1 mJ cm^{-2}. A small amount (~10%) of the Libra-output light was delivered to the measurement system (ExiPro, CDP Inc.) which utilized a sapphire plate as a White Light Continuum (WLC) generator to produce the probe beam. The probe beam was then split into two parts: the probe signal and probe reference beams (~0.1 mm diameter). The delay time limit for the machine is ~6 ns. The signal and reference beams were passed through the sample and their spectra were measured by monochromator with a pair of array detectors. The gap between the wavelength ranges is due to strong WLC distortions caused by the fundamental (800 nm) pulse of the Libra laser. The transient absorption spectra were obtained by comparing responses with and without excitation using a chopper synchronized with the fundamental laser pulses and blocking every second pump pulse. ExiPro Program (CDP Corp.) was used to control the experiment and calculate the spectra. The sample solutions for pump–probe measurements were prepared to have absorbance between 0.2–0.8 optical densities (OD) in 2 mm cuvette used for the measurements and equipped with magnetic stirred bar. The optical scheme was aligned for maximum overlap of the pump and prove signal through the whole cuvette thickness. Zero reference time was found by looking for the start of signal build-up, with the delay line first set for the pump pulse hitting the sample after the probe pulse and moving the delay line so that pump started to overlap the probe in time. Steady-state absorption spectra were

measured before and after the pump–probe measurement to confirm that the sample did not change during the measurement.

Author contributions

In this paper, Dr Lingli Zeng took responsibility for designing this project, performing the experiments, data analysis, writing up the paper and the grant application. Dr Dumitru Sirbu took part in the experimental and data processing part. Prof. Nikolai Tkachenko from Tampere University of Technology is the collaborator and provided technical support for using the femtosecond pump probe spectroscopy. Prof. Andrew Benniston is the corresponding author in the project and applied for the RSC Researcher Mobility Grant.

Conflicts of interest

There are no conflicts to declare.

Acknowledgements

We thank the Royal Society of Chemistry Researcher Mobility Grant for financial support. The National Mass Spectrometry Facility at Swansea University is also thanked for collecting mass spectra.

Notes and references

1 (*a*) Y. Li and J.-G. Jiang, *Food Funct.*, 2018, **9**, 6063–6080; (*b*) S. Siddamurthi, G. Gutti, S. Jana, A. Kumar and S. K. Singh, *Future Med. Chem.*, 2020, **12**, 1037–1069; (*c*) W. Tian, C. Wang, D. Li and H. Hou, *Future Med. Chem.*, 2020, **12**, 627–644.

2 (*a*) X. Dong, J. Fu, X. Yin, S. Cao, X. Li, L. Lin, Huyiligeqi and J. Ni, *Phytother. Res.*, 2016, **30**, 1207–1218; (*b*) M. R. Gerhardt, L. Tong, R. Gómez-Bombarelli, Q. Chen, M. P. Marshak, C. J. Galvin, A. Aspuru-Guzik, R. G. Gordon and M. J. Aziz, *Adv. Energy Mater.*, 2017, **7**, 1601488; (*c*) B. Hu, J. Luo, M. Hu, B. Yuan and T. L. Liu, *Angew. Chem.*, 2019, **131**, 16782–16789.

3 D. De Santis and M. Moresi, *Ind. Crops Prod.*, 2007, **26**, 151–162.

4 E. M. Malik and C. E. Müller, *Med. Res. Rev.*, 2016, **36**, 705–748.

5 L. Weisenthal, H. Liu and C. Rueff-Weisenthal, *Nat. Preced.*, 2010, 1–1.

6 (*a*) A. DelMedico, P. R. Auburn, E. S. Dodsworth, A. B. P. Lever and W. J. Pietro, *Inorg. Chem.*, 1994, **33**, 1583–1584; (*b*) A. DelMedico, S. S. Fielder, A. B. P. Lever and W. J. Pietro, *Inorg. Chem.*, 1995, **34**, 1507–1513.

7 L. Zeng, D. Sirbu, P. G. Waddell, N. V. Tkachenko, M. R. Probert and A. C. Benniston, *Dalton Trans.*, 2020, **49**, 13243–13252.

8 (*a*) Z. Zhao, X. Zhang, C.-e. Li and T. Chen, *Biomaterials*, 2019, **192**, 579–589; (*b*) V. Ramu, S. Gautam, P. Kondaiah and A. R. Chakravarty, *Inorg. Chem.*, 2019, **58**, 9067–9075; (*c*) P. Srivastava, K. Singh, M. Verma, S. Sivakumar and A. K. Patra, *Eur. J. Med. Chem.*, 2018, **144**, 243–254.

9 (*a*) H. Shi, T. Fang, Y. Tian, H. Huang and Y. Liu, *J. Mater. Chem. B*, 2016, **4**, 4746–4753; (*b*) M. Mariappan, R. Alagarsamy, A. P. Panneerselvam, A. Veerappan, S. Rajendran and J. Arunachalam, *J. Photochem. Photobiol., A*, 2018, **356**, 617–626; (*c*) A. N. Hidayatullah, E. Wachter, D. K. Heidary, S. Parkin and E. C. Glazer, *Inorg. Chem.*, 2014, **53**, 10030–10032.

10 M. I. Sánchez, G. Rama, R. Calo-Lapido, K. Ucar, P. Lincoln, M. Melle-Franco, J. L. Mascareñas and M. Eugenio Vázquez, *Chem. Sci.*, 2019, **10**, 8668–8674.

11 B. Kolp, H. Viebrock, A. von Zelewsky and D. Abeln, *Inorg. Chem.*, 2001, **40**, 1196–1198.

12 A. DelMedico, W. J. Pietro and A. B. P. Lever, *Inorg. Chim. Acta*, 1998, **281**, 126–133.

13 S. Yoon, P. Kukura, C. M. Stuart and R. A. Mathies, *Mol. Phys.*, 2006, **104**, 1275–1282.

14 M. Taniguchi and J. S. Lindsey, *Photochem. Photobiol.*, 2018, **94**, 290–327.

15 A. DelMedico, E. S. Dodsworth, A. B. P. Lever and W. J. Pietro, *Inorg. Chem.*, 2004, **43**, 2654–2671.

16 R. Englman and J. Jortner, *Mol. Phys.*, 1970, **18**, 145–164.

17 C. Creutz and N. Sutin, *Proc. Natl. Acad. Sci. U. S. A.*, 1975, **72**, 2858–2862.

18 A. Kytsya, L. Bazylyak, Y. Hrynda, A. Horechyy and Y. Medvedevdkikh, *Int. J. Chem. Kinet.*, 2015, **47**, 351–360.

19 J. Hankache, D. Hanss and O. S. Wenger, *J. Phys. Chem. A*, 2012, **116**, 3347–3358.

20 A. Babaei, P. A. Connor, A. J. McQuillan and S. Umapathy, *J. Chem. Educ.*, 1997, **74**, 1200–1204.

21 D. A. Armstrong, R. E. Huie, S. Lymar, W. H. Koppenol, G. Merényi, P. Neta, D. M. Stanbury, S. Steenken and P. Wardman, *BioInorg. React. Mech.*, 2013, **9**, 59–61.

22 C. Fotia, S. Avnet, D. Granchi and N. Baldini, *J. Orthop. Res.*, 2012, **30**, 1486–1492.

23 D. Bartusik, M. Minnis, G. Ghosh and A. Greer, *J. Org. Chem.*, 2013, **78**, 8537–8544.

24 (*a*) F. Abou-Chahine, D. Fujii, H. Imahori, H. Nakano, N. V. Tkachenko, Y. Matano and H. Lemmetyinen, *J. Phys. Chem. B*, 2015, **119**, 7328–7337; (*b*) D. Sirbu, C. Turta, A. C. Benniston, F. Abou-Chahine, H. Lemmetyinen, N. V. Tkachenko, C. Wood and E. Gibson, *RSC Adv.*, 2014, **4**, 22733–22742.